



## **Permeability, porosity, dispersion-, diffusion-, and sorption characteristics of chalk samples from Erslev, Mors, Denmark**

**Carlsen, L.; Pedersen, Walther Batsberg; Jensen, Bror Skytte; Bo, P.**

*Publication date:*  
1981

*Document Version*  
Publisher's PDF, also known as Version of record

[Link back to DTU Orbit](#)

*Citation (APA):*  
Carlsen, L., Pedersen, W. B., Jensen, B. S., & Bo, P. (1981). *Permeability, porosity, dispersion-, diffusion-, and sorption characteristics of chalk samples from Erslev, Mors, Denmark*. Risø National Laboratory. Denmark. Forskningscenter Risoe. Risoe-R No. 451

---

### **General rights**

Copyright and moral rights for the publications made accessible in the public portal are retained by the authors and/or other copyright owners and it is a condition of accessing publications that users recognise and abide by the legal requirements associated with these rights.

- Users may download and print one copy of any publication from the public portal for the purpose of private study or research.
- You may not further distribute the material or use it for any profit-making activity or commercial gain
- You may freely distribute the URL identifying the publication in the public portal

If you believe that this document breaches copyright please contact us providing details, and we will remove access to the work immediately and investigate your claim.



# **Permeability, Porosity, Dispersion-, Diffusion-, and Sorption Characteristics of Chalk Samples from Erslev, Mors, Denmark**

**Lars Carlsen, Walther Batsberg, Bror Skytte Jensen, and  
Peter Bo**

**Risø National Laboratory, DK-4000 Roskilde, Denmark  
August 1981**

RISØ-R-451

PERMEABILITY, POROSITY, DISPERSION-, DIFFUSION-, AND SORPTION  
CHARACTERISTICS OF CHALK SAMPLES FROM ERSLEV, MORS, DENMARK

Lars Carlsen, Walther Batsberg, Bror Skytte Jensen, and Peter Bo  
Chemistry Department

Abstract. A series of chalk samples from the cretaceous formation overlying the Erslev salt dome have been studied in order to establish permeabilities, porosities, dispersion-, diffusion-, and sorption characteristics of the chalk. Predominantly the investigations have been carried out by application of a liquid chromatographic technique.

The chalk was found to be porous ( $\epsilon \approx 0.4$ ), however, of rather low permeability ( $k \approx 10^{-7}$  cm/sec). It was found that the material exhibits a retarding effect on the migration of cationic

(continue on next page)

August 1981

Risø National Laboratory, DK 4000 Roskilde, Denmark

species as  $\text{Cs}^+$ ,  $\text{Sr}^{2+}$ ,  $\text{Co}^{2+}$ , and  $\text{Eu}^{3+}$ , whereas anionic species as  $\text{Cl}^-$  and  $\text{TcO}_4^-$  move with the water front.

The geochemical implications are discussed.

INIS descriptors: ADSORPTION; CALCIUM CARBONATES; CESIUM 134; CESIUM COMPOUNDS; CHALK; CHLORINE 36; CHLORINE COMPOUNDS; COBALT 60; COBALT COMPOUNDS; DIFFUSION; EUROPIUM 154; EUROPIUM COMPOUNDS; EXPERIMENTAL DATA; FLOW RATE; GEOCHEMISTRY; ION EXCHANGE; LIQUID COLUMN CHROMATOGRAPHY; MIGRATION LENGTH; PERMEABILITY; PERTECHNETATES; POROSITY; POROUS MATERIALS; RADIOISOTOPES; RADIO-NUCLIDE; MIGRATION; STRONTIUM 85; STRONTIUM COMPOUNDS; TECHNETIUM 99; WATER.

UDC 552.54

ISBN 87-550-0785-6

ISSN 0106-2840

Risø Repro 1981

## CONTENTS

	Page
1. INTRODUCTION .....	5
2. BASIC PRINCIPLES OF LIQUID CHROMATOGRAPHY .....	6
3. EXPERIMENTAL .....	10
3.1. Preparation of Chalk columns .....	10
3.2. Liquid chromatography equipment .....	11
3.3. Density determinations .....	12
3.4. Retention data by batch-type experiments .....	13
4. RESULTS .....	14
4.1. Permeability .....	14
4.2. Porosity .....	17
4.3. Dispersion .....	20
4.4. Diffusion coefficients .....	21
4.5. Sorption phenomena .....	25
5. GEOCHEMICAL IMPLICATIONS .....	38
5.1. Redox and pH conditions in the Erslev chalk formation .....	38
5.2. Geochemistry of radionuclides .....	42
6. CONCLUSIONS .....	44
ACKNOWLEDGMENTS .....	46
REFERENCES .....	46



## 1. INTRODUCTION

In connection with the possible disposal of nuclear waste in the salt dome located at Erslev, Mors, Denmark, a physico-chemical characterization of the chalk formation overlying the salt dome has been undertaken.

The chalk samples investigated in the present study originates from the Erslev wells ERSLEV 1S, ERSLEV 2S, ERSLEV 3S, and ERSLEV 4S, respectively. The samples were received from the Danish Geological Survey (DGU). A detailed geological characterization of the chalk formation has been performed by DGU, the results being described elsewhere.\*)

In the present study a series of physico-chemical measurements on the chalk samples (in total 21 samples have been investigated) including determinations of permeabilities, porosities, dispersion, and sorption characteristics are reported, supplementary with a discussion of the results obtained. In addition a discussion of the possible geochemical implications of the derived data is given.

In the major part of the experiments a modified liquid chromatographic technique has been applied to determine permeability, porosity, dispersion, and retention data for the chalk samples. Additionally, the porosities have also been calculated on the basis of density measurements, and the sorption phenomena studied by batch type experiments.

---

\*) The geological characterization of the Erslev chalk formation has been reported by the Danish Geological Survey as a contribution to the ELSAM/ELKRAFT management project, phase 2.

## 2. BASIC PRINCIPLES OF LIQUID CHROMATOGRAPHY (LC)

Liquid chromatography is a column technique used for the separation of different organic as well as inorganic components in a solution. The separation mechanism depends on the nature of the physical/chemical interaction between the solute and the column packing material. For a given column material, e.g. chalk, the separation mechanism will be controlled by adsorption as well as ion-exchange processes. As eluent flow through the column, different solutes can selectively be retarded, but still eluted. A chromatogram is obtained when the outlet from the column is monitored by a e.g. refractive index detector or a radioactivity monitor. A typical experimental set up for a liquid chromatographic separation is visualized in Fig. 1.

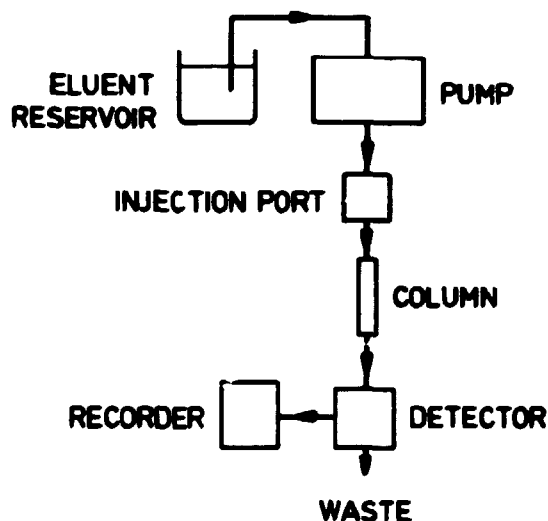


Fig. 1. Experimental liquid chromatography set up.

The pump delivers a solvent (eluent) flow at a preset constant flow rate. A sample of known volume is injected into the column via the injection port, and the actual composition of the eluate from the column is examined by the detector.



Based on the appearance of the chromatogram a variety of physico-chemical characteristics for the column can be calculated.

The PERMEABILITY,  $K$ , for a given column is determined by the volume flow rate,  $Q$  ( $\text{cm}^3/\text{sec}$ ), the length of the column,  $l$  (m), the cross sectional area of the column,  $A$  ( $\text{cm}^2$ ), and the pressure drop over the column,  $h$  (metre of water) (Eq. 2.1) (Dahl, 1979).

$$K = Q \cdot l / A \cdot h \quad (\text{cm/sec}) \quad (2.1)$$

The volume porosity,  $\epsilon$ , of the column can be determined by injection of a solute, which is not retarded by the column packing material (Eq. 2.2)

$$\epsilon = V_0 / A \cdot l \quad (2.2)$$

where  $V_0$  is the so-called dead volume (cf. Fig. 2).

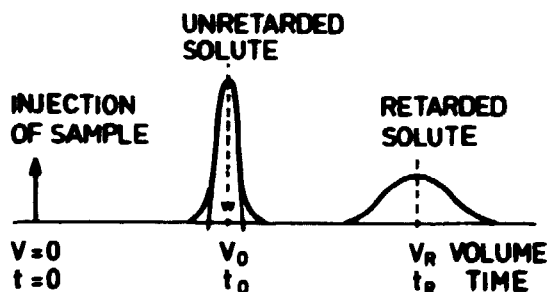


**Fig. 2.** Schematic chromatogram defining the elution volume ( $V_0$ ) and elution time ( $t_0$ ) for the unretarded solute and the retention volume ( $V_R$ ) and retention time ( $t_R$ ) for a retarded solute.

The shape of the peak corresponding to an unretarded solute characterizes the flow dispersion in the column, whereas the elution volume (or elution time) and shape for a retarded peak (cf. Fig. 2) characterizes the sorption phenomena, related to the solute under investigation, to the column packing material.

The FLOW DISPERSION,  $\sigma$ , is determined from the width of the chromatogram,  $w$ , measured at the base line. For a chromatogram, exhi-

biting a Gaussian distribution with a standard deviation,  $\sigma$ , the  $\sigma$ -w dependence is given by Eq. 2.3 (Yau, Kirkland and Bly, 1979).

$$w = 4 \cdot \sigma \quad (2.3)$$

The RETENTION FACTOR is determined according to Eq. 2.4 (cf. Fig. 2)

$$R_f = V_O/V_R = t_O/t_R \quad (2.4)$$

The sorption ability of a given column packing material is in general expressed by the distribution coefficients,  $K_D$ , for the solute M (Eq. 2.5)

$$K_D = \bar{c}_M/c_M \quad (2.5)$$

where  $\bar{c}_M$  and  $c_M$  are the concentrations of M on the solid phase and in solution, respectively. The  $K_D$  values are related to the retention factors by the expression given in Eq. 2.6

$$R_f = (1 + (1-\epsilon) \cdot \rho \cdot K_D / \epsilon)^{-1} \quad (2.6)$$

Where  $\epsilon$  is the above mentioned volume porosity and  $\rho$  is the bulk density of the solid phase. The retention factors reflect the movement of M relative to the solvent front.

In the major part of the experiments reported here the LC-technique are applied to so-called homogeneous columns consisting of undisturbed chalk samples (cf. experimental section), and the solutes are selected so that both the sorption properties of relevant radionuclides as well as some hydraulic parameters of consolidated chalk from Erslev can be determined.

However, although studies of retention phenomena in principle can be performed on homogeneous columns, it shall be emphasized that retention times,  $t_R$ , higher than 10 - 15 times the dead time,  $t_O$ , of the column (i.e. retention factors less than ca. 0.07) afford unsatisfactory broad peaks, which at the limit may

escape detection. For the study of sorption phenomena, resulting in retention factors less than ca. 0.07 so-called heterogeneous columns may advantageously be used. These columns consist of a known amount of crushed material, which sorption characteristics is to be investigated, mixed with "hydrophilic" polystyrene spheres with a mean particle diameter less than 160  $\mu\text{m}$ , the latter exhibiting no retarding effect towards the radionuclides studied in the present study. Since the retarding effect of these "diluted" columns apparently is considerable less than that of the corresponding homogeneous columns, these types of experiments enable us to study the retention of radionuclides with much smaller retention factors than do those with the homogeneous columns.

It is important to note that the study of retention phenomena in the heterogeneous columns give rise to determination of apparent retention factors,  $R_f^{\text{obs}}$ , according to Eq. 2.4. It shall, however, be emphasized that the true retention factors,  $R_f$ , corresponding to the retention in a column consisting of undiluted, undisturbed sorbing material, are not directly obtainable, since the dilution with non-sorbing material affords a decrease in the apparent distribution coefficients,  $K_D^{\text{obs}}$ , proportional to the dilution (Eq. 2.7)

$$K_D^{\text{obs}} = K_D \cdot a^{-1} \quad (2.7)$$

where  $K_D^{\text{obs}}$  is the distribution coefficient in the diluted material and  $a$  is the dilution factor ( $a \geq 1$ ; in the present study dilution factors between 10 and 20 have been applied).

By analogy with Eq. 2.6 the connection between  $R_f^{\text{obs}}$  and  $K_D^{\text{obs}}$  is given by Eq. 2.8

$$R_f^{\text{obs}} = (1 + (1 - \epsilon') \cdot \rho' \cdot K_D^{\text{obs}} / \epsilon')^{-1} \quad (2.8)$$

which may be rewritten into the following expression for  $K_D^{\text{obs}}$  (Eq. 2.9)

$$K_D^{\text{obs}} = ((1 - R_f^{\text{obs}}) / R_f^{\text{obs}}) \cdot \epsilon' / (1 - \epsilon') \cdot \rho' \quad (2.9)$$

$\epsilon'$  and  $\rho'$  are porosity and bulk density of the heterogeneous column. Combining 2.7 and 2.9 we obtain the expression (Eq. 2.10) for the true distribution coefficient

$$K_D = a \cdot (\epsilon' / \rho' (1 - \epsilon')) (1 - R_f^{\text{obs}}) / R_f^{\text{obs}} \quad (2.10)$$

The true retention factor can be calculated according to Eq. 2.6. It should be noted that  $R_f$  factors determined dynamically by use of heterogeneous columns correspond to retention factors on pure crushed material, and may differ from the true values in the consolidated material (cf. the discussion on batch type vs. column type experiments in section 4.5).

### 3. EXPERIMENTAL

The chalk samples were received from the Danish Geological Survey as cylindrical specimens with a diameter approximately 10 cm and a length of approximately 12 cm. Some of the samples were waxed and wrapped in a heavy polyethylene foil, others only packed in polyethylene foil.

#### 3.1. Preparation of chalk columns

Immediately after unwrapping, the cylindrical specimen was cut twice using a band saw. Two half cylinders and a rectangular plate with nearly the same dimensions as the length and the diameter of the cylinder were obtained. A small part of the plate was used for the chemical analyses and water determinations (Solgård and Skytte Jensen, 1981). From the remaining part of the plate, rods with the dimensions  $120 \times 12 \times 12 \text{ mm}^3$  were cut either parallel or perpendicular to the cylinder axis. The rod was mounted in a lathe and while rotating polished to cylindrical rods with a diameter of 10 mm. Finally, they were cut to the length of 100 mm, 50 mm, or 10 mm.

Before use in a column experiment the cylindrical chalk rod was provided with end fittings of polyethylene, porous metal and glass fiber filters and encapsulated in a heat shrinkable tubing with a diameter of 12.5 mm. After heat shrinking of the tubing, the column was further encapsulated in another heat shrinkable tubing. After heat shrinking the total outer diameter of the column was approximately 12.5 mm (cf. Fig. 3).

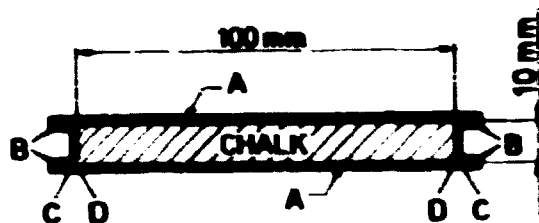


Fig. 3. Chalk column. A: two layers of polyethylene, B: polyethylene end-fittings, C: porous metal filters, and D: porous glass fiber filters.

Occasionally it was impossible to cut out a rod with a total length of 100 mm, in which cases the columns were made of more than one piece. For samples with very low permeabilities or for the determinations of retention factors, the total length of the samples was reduced to 50 mm or 10 mm. In these cases cylindrical teflon rods with a bore of 1.5 mm were used as spacers in order to retain the total length of the column.

### 3.2. Liquid chromatography equipment

For the determination of permeability, pore volume and dispersion a high pressure pump, model PR-30, KNAUER KG, Berlin, BRD, an injection port, model 7120, Rheodyne, California, USA, provided with a 20  $\mu$ L loop, a compression module, RCM-100, Waters Ass., Mass., USA, retrofitted with an accurate manometer, and a refractive index detector, model R-401, Waters Ass., Mass., USA, were used (cf. Fig. 1). For the retention measurements the KNAUER pump was substituted with a Kontron pump, model LC-410, and the detector was a radioactivity monitor LB-503, Dr. Berthold, Wildbad, BRD. The injection port was for the retention measurements provided with a 50  $\mu$ L loop. In both cases a BD-9 recorder, Kipp-

Zonen, was used and the flow rate was determined by collecting the eluate in a graduated cylinder for a given time.

The experiments were performed in the following way: The chalk column was inserted in the RCM-100 compression module (cf. Fig. 4), and a hydrostatic pressure on the column was generated by activating the different levers. Redistilled water or salt solutions was pumped through the column. The flow rate was adjusted so that the hydrostatic pressure in the compression module was higher than the pressure drop over the column. Before injection of the solutes the column was equilibrated until a stable base line of the detector signal was obtained.

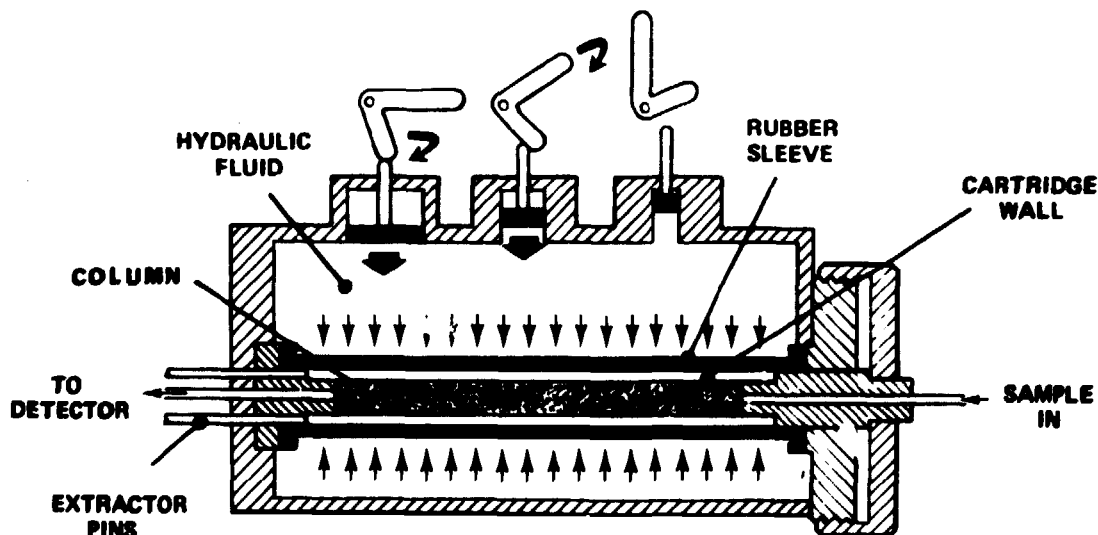


Fig. 4. RCM-100 Compression Module. Lowering the levers applies pressure to the column (courtesy of Waters Ass., Denmark).

### 3.3. Density determinations

The densities of the chalk samples were determined by weighing the samples in air and immersed in redistilled water. Before weighing the samples were equilibrated overnight in redistilled water.

### 3.4. Retention data by batch-type experiments

Dry crushed samples (ca. 250 mg) were equilibrated in centrifuge tubes for 1 hour with 26 mL of a salt solution (salt solution A: 25 mL 1M NaCl + 1 mL radionuclide solution; salt solution B: 25 mL 5M NaCl + 1 mL radionuclide solution. The radionuclide solution contains  $\text{Eu}^{3+}$ ,  $\text{Sr}^{2+}$ ,  $\text{Co}^{2+}$ , and  $\text{Cs}^{+}$ , all in concentrations of ca.  $2.5 \cdot 10^{-2}$  eq/L, and trace amounts of  $^{154}\text{Eu}^{3+}$ ,  $^{85}\text{Sr}^{2+}$ ,  $^{60}\text{Co}^{2+}$ , and  $^{134}\text{Cs}^{+}$ , corresponding to ca. 0.2  $\mu\text{Ci/mL}$ ).

After centrifugation ( $\frac{1}{2}$  h) 10 mL of the supernatants were transferred into counting bottles; the remaining supernatant was removed by decantation. The moist chalk samples were weighed in order to correct for the amount of solution which cannot be removed in this way. The moist chalk samples were then dissolved in 10 mL 2M hydrochloric acid, the resulting solution being transferred to counting bottles.

The samples (supernatant and chalk) were then counted on ND-100 multichannel analyzer using Ge(Li) detector ( $^{154}\text{Eu}$ : 122 keV,  $^{85}\text{Sr}$ : 513 keV,  $^{134}\text{Cs}$ : 604 keV,  $^{60}\text{Co}$ : 1173 keV). Distribution coefficients were calculated according to Eq. 3.1

$$K_D = \frac{10(A_{\text{chalk}} - A_{\text{sol}} \cdot (W_{\text{c,m}} - W_{\text{c,d}})/10)}{W_{\text{c,d}} \cdot A_{\text{sol}}} \text{ mL/g} \quad (3.1)$$

where  $W_{\text{c,d}}$  and  $W_{\text{c,m}}$  are the weights of the dry and moist chalk samples, respectively, and  $A_{\text{chalk}}$  and  $A_{\text{sol}}$  are the radioactivity (counts/1000 sec.) for the dissolved chalk samples and 10 mL of the supernatant, respectively.

The calculations of  $K_D$  values are carried out separately for each of the four nuclides.

All determinations were carried out in duplicate.

## 4. RESULTS

In the following section the results for permeability, porosity, dispersion, diffusion, and retention will be given separately.

### 4.1. Permeability

The permeability is calculated from Eq. 2.1. Correct values of the permeability is obtained if the presence of voids or channels at the interface between the chalk rod and the polyethylene tubing can be excluded. This will be the case when the hydrostatic pressure in the compression module is higher than the pressure drop over the column. In Table 1 the permeabilities as function of flow rate and hydrostatic pressure for a given chalk column is given.

Table 1. Permeability (K), volume porosity ( $\epsilon$ ), and dispersion ( $\sigma$ ) as function of hydrostatic pressure ( $P_y$ ) and pressure drop ( $P_i$ ) over 100 mm Erslev 1s-5 column.

$P_y$	$P_i$	flow rate	permeability	volume porosity	dispersion
bar	bar	mL/min	cm/sec	%	$\sigma$
40	21	0.101	$1.02 \cdot 10^{-6}$	40.5	0.052
42	31	0.167	$1.14 \cdot 10^{-6}$	40.2	0.058
46	42	0.235	$1.19 \cdot 10^{-6}$	41.1	0.056
56	52	0.293	$1.20 \cdot 10^{-6}$	40.1	0.061
66	70	0.360	$1.09 \cdot 10^{-6}$	39.7	0.065
84	33	0.170	$1.09 \cdot 10^{-6}$	41.4	0.058
84	78	0.360	$1.00 \cdot 10^{-6}$	41.3	0.059
133	66	0.167	$0.55 \cdot 10^{-6}$	38.3	0.053
145	135	0.360	$0.57 \cdot 10^{-6}$	38.0	0.051

The results (Table 1) show that the permeability is nearly independent of the pressure drop over the column over a wide range of flow rates. If very high hydrostatic pressures are applied,



the permeability appears to decrease slightly. A similar trend is observed in the values for the pore volume and the dispersion.

The permeabilities as determined for all 21 chalk samples available are visualized in Fig. 5 and 6 as function of depth below ground level. All data were obtained at flow rates where  $P_y > P_i$ .

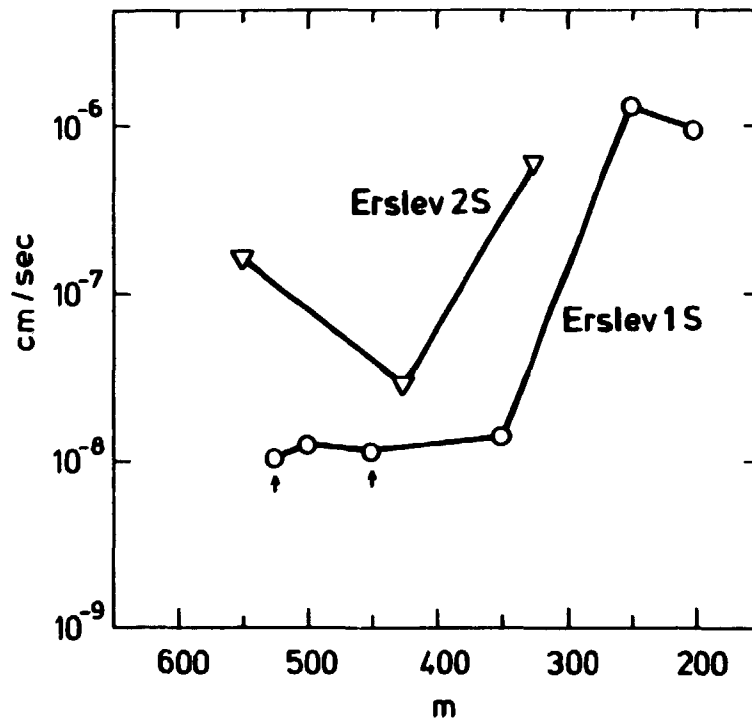


Fig. 5. Permeabilities as function of depth for chalk samples from Erslev 1s and 2s.

All samples except the two marked † were cut perpendicular to the well direction. The permeability of each of the two samples (Erslev 1s-10 and Erslev 1s-12), cut parallel to the well direction, is comparable to that for a sample from Erslev 1s-11.

Supplementary, a determination of the possible change in permeability as function of time for a column exhibiting a well defined crack was performed. The first 30 mm of the column in the direction of the flow was a normal consolidated cylindrical rod, whereas the next 70 mm was made of two half cylinders. As the

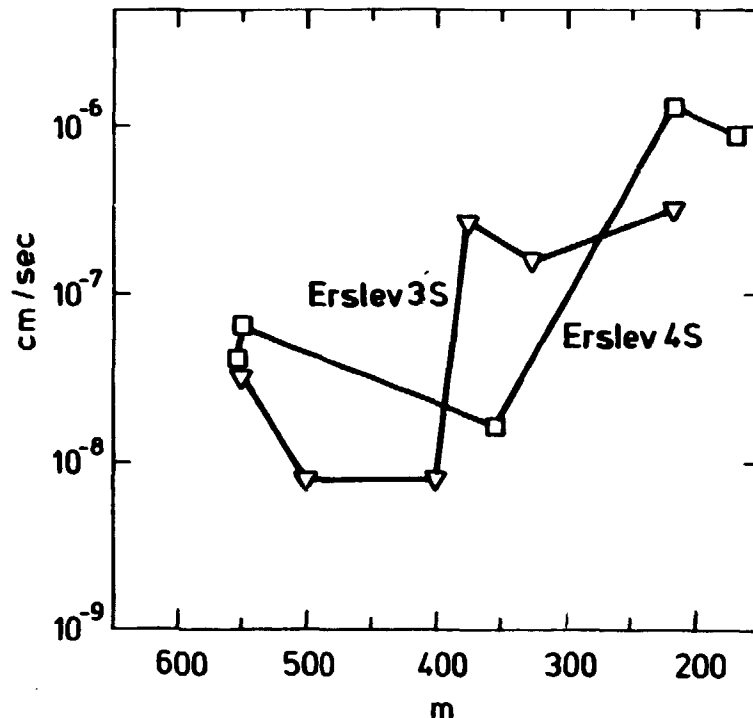


Fig. 6. Permeabilities as function of depth for chalk samples from Erslev 3s and 4s.

eluent (redistilled water partially saturated with calcium carbonate) was passed through the first 30 mm, a further saturation of the eluent with  $\text{CaCO}_3$  was assumed to occur. The hydrostatic pressure on the column was approximately 100 bar through out the experiment. The permeability was determined at different times, and the results are given in Table 2.

At the end of the experiment (160 hours) approximately 600 mL eluent have been passed through the column, corresponding to ca. 150 times the pore volume in the column. Only minor variations in the permeability is observed. Especially the surprisingly low initial permeability should be noted.

**Table 2.** Permeability of a chalk column initially containing a well defined, macroscopic crack. (Erslev 4s-3, flow rate: ca. 0.06 mL/min.,  $P_y$  ca. 100 bar,  $P_i$  ca. 30 bar)

time (after start of exp.)	permeability
hours	cm/sec.
0	$5.7 \cdot 10^{-7}$
30	$4.2 \cdot 10^{-7}$
45	$4.7 \cdot 10^{-7}$
117	$4.5 \cdot 10^{-7}$
140	$5.3 \cdot 10^{-7}$
160	$4.7 \cdot 10^{-7}$

#### 4.2. Porosity

The pore volumes of the chalk columns was determined from a chromatogram obtained after injection of a 20  $\mu$ L sample containing 30%  $D_2O$  (cf. Fig. 7). It is assumed that  $D_2O$  is not retarded in the chalk columns, equilibrated with  $H_2O$  before the injection of the  $D_2O/H_2O$  sample. However, if the permeability of the column is less than ca.  $10^{-7}$  cm/sec. the flow rate through the column

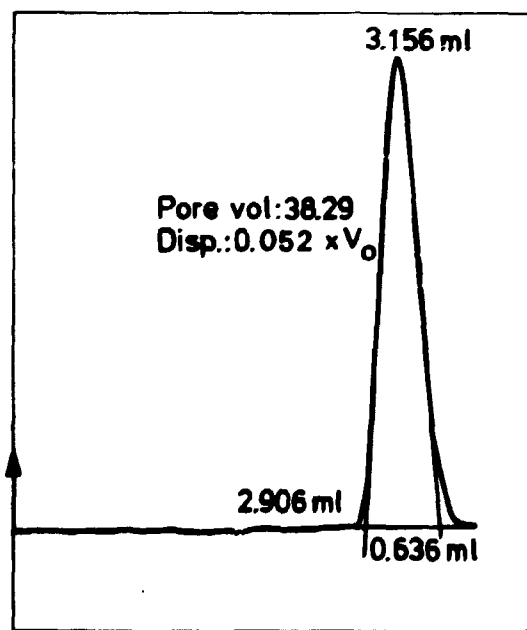


**Fig. 7.** Determination of pore-volume and dispersion from the chromatogram of a  $D_2O$  solution (10 cm Erslev 1s-5 column (flow rate 0.167 mL/min., chart speed 0.5 cm/min.)).

is so low that lack of stability of the refractive index detector for the long elution times needed seems to be prohibitive for a good determination of the pore volume. Hence, the elution times can be reduced by introduction of a shorter column (50 mm or 10 mm), however, excessive external volumes (e.g. dead volume in the spacers, cf. Experimental section) have to be taken into account.

For columns with low permeabilities the pore volume can advantageously be determined by injection of a radioactive sample, e.g.  $^{36}\text{Cl}^-$ , which will not be retarded on the column, and subsequent detection with a radioactivity monitor.

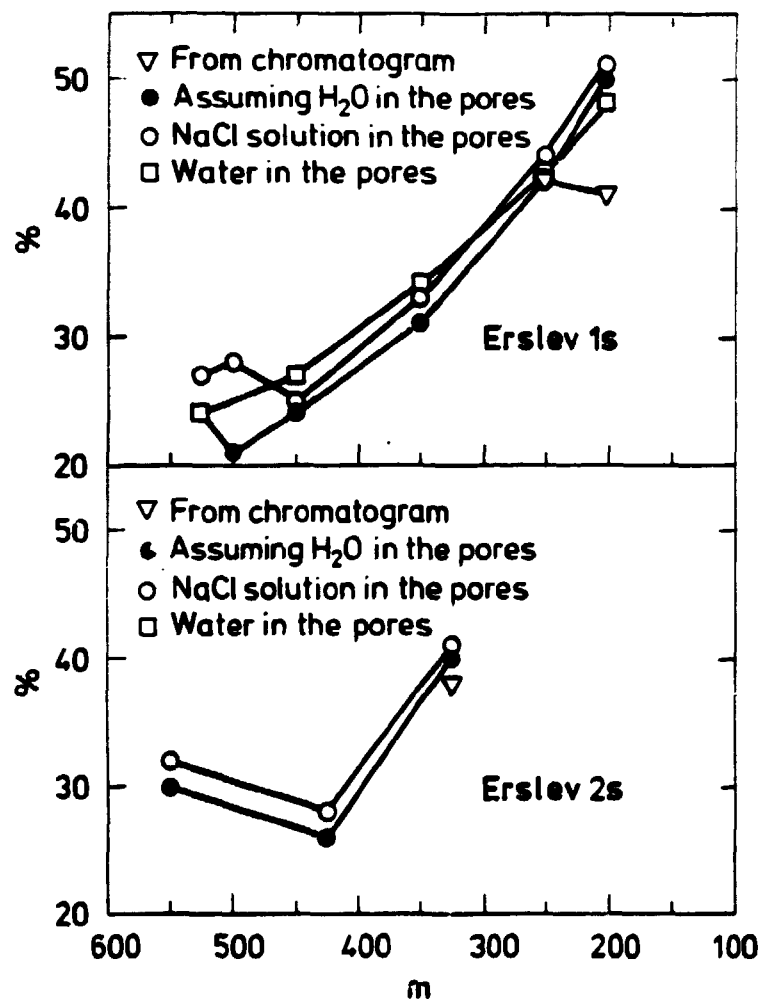


**Fig. 8.** Porosities as function of depth for chalk samples from Erslev 1s and 2s.

Porosities were additionally determined from density measurements on chalk samples with the original salt solution in the pores or with redistilled water in the pores (i.e. samples primarily used for permeability measurements were applied here). The porosities were calculated assuming the density of non-porous  $\text{CaCO}_3$  to be  $2.7 \text{ g/cm}^3$ , and a density of the original salt solution of  $1.00 \text{ g/cm}^3$ . Complementary, the actual density of the salt solution originally present in the pores, the molarity being established in a supplementary study (Solgård and Skytte Jensen, 1981), was used. In Fig. 8 and 9 the results are summarized.

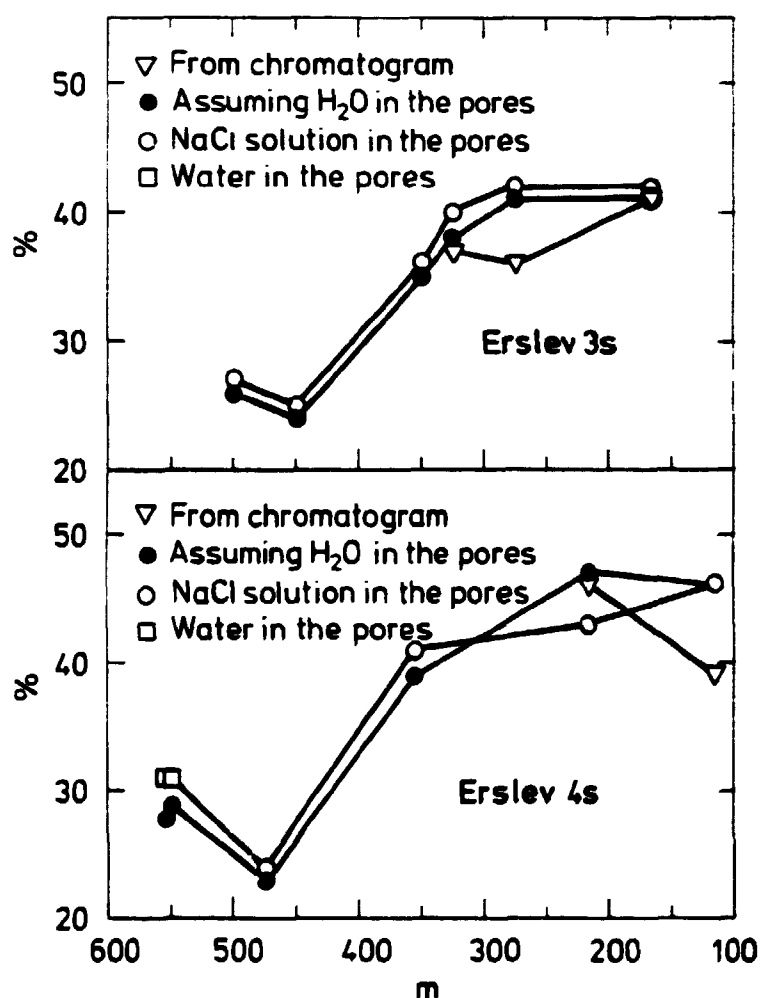


Fig. 9. Porosities as function of depth for chalk samples from Erslev 3s and 4s.

It is noted that a good agreement between the "NaCl" (o) and the "H<sub>2</sub>O" (u) results is obtained. The porosities determined from the chromatogram are in general somewhat lower.

#### 4.3. Dispersion

In Table 1 the dispersion as function of flow rate for a 100 mm Erslev 1s-5 column is given, the standard deviation of the chromatogram,  $\sigma$ , being calculated in units of the pore volume,  $V_0$ . (Fig. 7)

If the dispersion observed is due to diffusion only, the Einstein-Smoluchowski relation (Eq. 4.1) is valid (Atkins, 1978).

$$\sigma \cdot L = \sqrt{2D \cdot t} \quad (4.1)$$

where  $L$  is the length of the column,  $D$  is the diffusion coefficient of  $D_2O$  in  $H_2O$ , and  $t$  is the retention time. Inserting the actual values,  $L = 10$  cm,  $\sigma = 0.052$ , and  $t = 31.5$  min into Eq. 4.1 the diffusion coefficient  $D$  is calculated to be  $7 \cdot 10^{-5}$  cm<sup>2</sup>/sec, which is somewhat higher than the generally accepted values for self diffusion in water ( $10^{-5}$  cm<sup>2</sup>/sec). However, corrections due to dispersion phenomena in the injection system, the connecting tubings, and the detector systems have to be taken into account. Hence, the corrected value is calculated to be  $6.2 \cdot 10^{-5}$  cm<sup>2</sup>/sec, on which background we are forced to conclude that other processes than diffusion contributed to the dispersion of  $D_2O$  in the chalk column at the flow rates examined ( $>0.03$  mL/min). An identical result is obtained after injection of the non-retarded radionuclide  $^{36}Cl^-$  followed by monitoring the eluate with a radioactivity detector. It should in this connection be emphasised that the lower limit of flow rate by these experiments (0.03 mL/min) most surely far exceed the actual flow rate in the chalk formation, and that a further lowering of the flow rate through the chalk columns is assumed to afford a subsequent decrease in the dispersion coefficient. Due to the very low permeabilities the effective diffusion coefficient of elements in the pore water is believed to be up to several orders of magnitude below the diffusion coefficient in pure water ( $10^{-5}$  cm<sup>2</sup>/sec).

#### 4.4. Diffusion coefficients

In the present study determination of the diffusion coefficients for sodium ions have been determined for two representative chalk samples, Erslev 3s-6 (-325 m) and Erslev 4s-7 (-552 m ), respectively.

##### 4.4.1. Diffusion in porous media

In porous media the apparent diffusion coefficient,  $D$ , measured relative to the open ends of a pore, is less than the intrinsic diffusion coefficient in the pore fluid by a factor equal to the square of the tortuosity of the pore, since the actual path is increased proportionally to the tortuosity, whereas the concentration gradient along the pore is reduced proportionally to the tortuosity. According to the theory of Mackie and Meares the apparent diffusion coefficient,  $D$ , is given by the empirical Eq. 4.2, where  $D_{aq}$  refers to the diffusion coefficient in pure water (Meares, 1968).

$$D = D_{aq} (\epsilon / (2 - \epsilon))^2 \quad (4.2)$$

$\epsilon$  is the porosity of the media.

However, it should be emphasized that the Eq. 4.2 applies to homogeneous media and only when the pore diameter is large compared to the diameter of the diffusion molecule.

A distinct decreasing effect of the apparent diffusion coefficient with decreasing pore size has been observed (Beck and Schultz, 1970), leading to a revised version of the above equation for  $D$ , given by Eq. 4.3.

$$D = D_{aq} \cdot Q \cdot (\epsilon / (2 - \epsilon))^2 \quad (4.3)$$

where  $Q$  is a constant less than 1. The actual magnitude of  $Q$  is solely dependent of the nature of the porous media and the diffusing material. In the present case it will accordingly be expected that for a given chalk sample, the factor  $Q$  will decrease

with increasing size of the diffusing ions. Analogously it will be expected that  $Q$  will decrease for a given ion, if the pore size of the chalk samples investigated decreases, i.e. the permeability of the samples decreases.

#### 4.4.2. Diffusion coefficients in pure water

The diffusion coefficients for ions,  $i$ , in pure water,  $D_{aq}^i$ , can be determined by application of the limiting ionic conductances,  $\lambda_i$  ( $\Omega^{-1} \text{ cm}^2$ ), in water (Eq. 4.4) (Harned and Owen, 1963)

$$D_{aq}^i = \lambda_i RT / |z_i|^2 F^2 \quad (\text{cm}^2 \text{s}^{-1}) \quad (4.4)$$

where  $R$  is the gas constant,  $T$  is the absolute temperature,  $z_i$  is the ionic charge, and  $F$  is the Faraday.

According to Eq. 4.4 the diffusion coefficients of sodium ions in water at room temperature can be calculated to be  $1.33 \cdot 10^{-5} \text{ cm}^2 \text{s}^{-1}$ .

#### 4.4.3. Apparent diffusion coefficients in chalk samples

For diffusion coefficient measurements the column in the liquid chromatographic system, described above, was substituted by a "diffusion unit" (Fig. 10) consisting of a 6 mL reservoir (filled with eluent) through which the eluent can be passed with a preset flow rate. At the top of the diffusion unit the column, still encapsulated in the shrinkable polyethylene tubing is placed as visualized in Fig. 10. However, the end fittings in the one end were removed, to ensure a free chalk surface in contact with the eluent in the reservoir, i.e. the contact area equals the cross sectional area of the chalk column. The upper end of the column is closed in order to prevent a possible flow up through the column. The eluent in the reservoir is stirred to ensure a uniform concentration within the total volume and avoid concentration polarization at the surface of the chalk. The variations in concentration in the reservoir as a result of a diffusive leaching from the column is followed by the detector by passing eluent slowly through the diffusion unit.



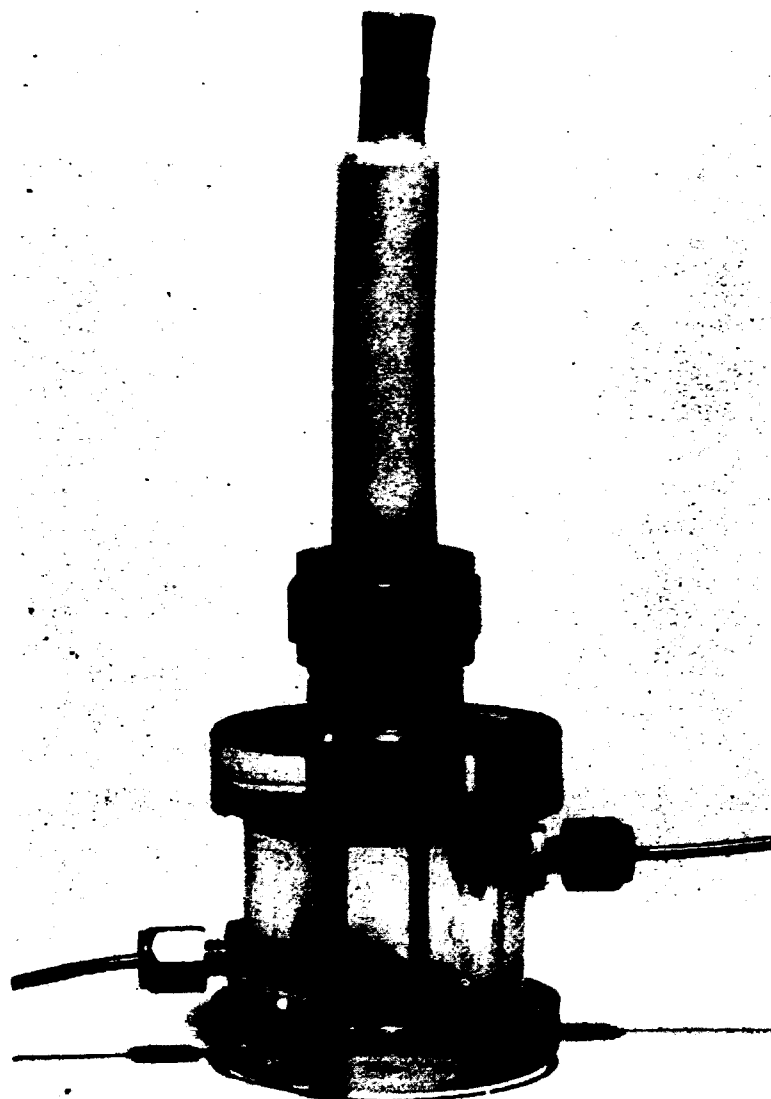


Fig. 10. Diffusion unit.

In the present case the chalk columns were, prior to the diffusion experiments saturated with a 1M NaCl solution containing  $^{22}\text{Na}^+$ , using the above described liquid chromatographic system. The diffusion unit was eluted with pure 1M NaCl, and the variations in  $^{22}\text{Na}^+$  in the reservoir were followed by the radioactivity monitor. No sorption of  $^{22}\text{Na}^+$  on the chalk was observed, possibly due to the high sodium concentration in the liquid phase.

The concentration variations obtained in this way were then simulated by application of the computer program DIFMIG (Bo and Carlsen, 1981a), which is designed to handle diffusive migration of radionuclides through column systems. In order to obtain satisfactory simulations it was necessary to include diffusion coefficients in the near surface region of the column (up to 1 mm) which are somewhat higher than the actual diffusion coefficient used for inner part of the column, presumably due to surface imperfections.

The apparent diffusion coefficients,  $D$ , for  $^{22}\text{Na}^+$  have been determined for two representative chalk samples from the Erslev formation. The results are summarized in Table 3, the data for the porosities,  $\epsilon$  and permeability,  $K$ , being adopted from above.

**Table 3.** Diffusion data for chalk samples from the Erslev formation.

sample	$\epsilon$	$K \text{ (cm s}^{-1}\text{)}$	$D \text{ (cm}^2 \text{ s}^{-1}\text{)}$
Erslev 3s-6	0.4	$1.6 \cdot 10^{-7}$	$5.0 \cdot 10^{-8}$
Erslev 4s-7	0.3	$1.7 \cdot 10^{-8}$	$1.7 \cdot 10^{-8}$

Fig. 11 shows the experimentally obtained variation in  $^{22}\text{Na}^+$  concentration ( $V$ ) and the corresponding DIFMIG simulation.

For the two chalk samples the diffusion coefficients in the near surface region were: Erslev 3s-6:  $3.4 \cdot 10^{-6} \text{ cm}^2 \text{ s}^{-1}$  (0-0.4 mm) and  $2.2 \cdot 10^{-6} \text{ cm}^2 \text{ s}^{-1}$  (0.4-0.8 mm). Erslev 4s-6:  $1.2 \cdot 10^{-6} \text{ cm}^2 \text{ s}^{-1}$  (0-0.4 mm) and  $1.0 \cdot 10^{-6} \text{ cm}^2 \text{ s}^{-1}$  (0.4-0.8 mm). As seen these coefficients vary, as expected, with the column used and are not expected to be reproducible, owing to differences in surfaces as a result of the handling of the individual samples. They should, however, always be less than the intrinsic diffusion coefficients of  $^{22}\text{Na}^+$  in pure water.

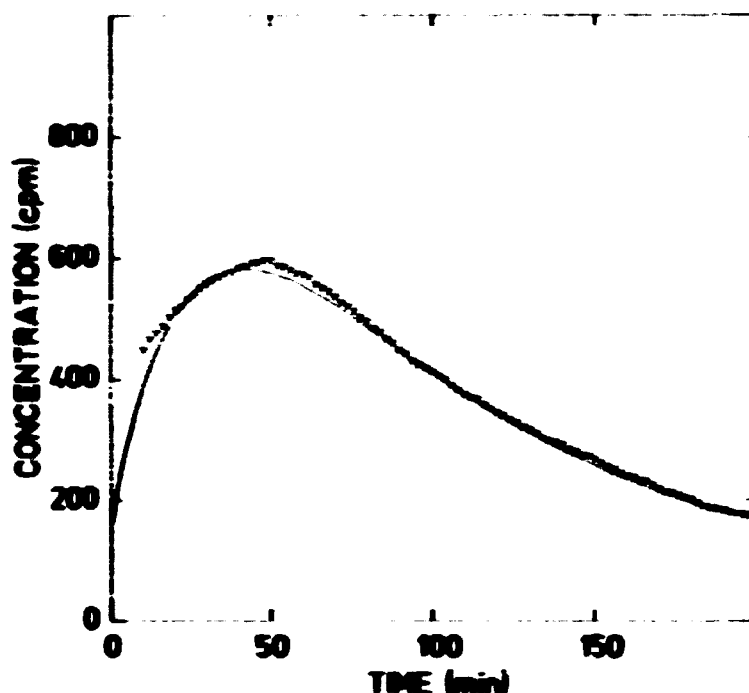


Fig. 11. Diffusive leaching of  $^{22}\text{Na}^+$  from a 10 cm Erslev 3s-6 column. Experimentally determined concentrations of the leachate (expressed in cpm) are given by V, the solid curve being the theoretical simulation by DIFFUG.

From the above data (Table 3) it is possible to estimate the factor  $Q$  (cf. Eq. 4.3). For the Erslev 3s-6 and Erslev 4s-7 the factor  $Q$  were determined to be 0.062 and 0.042, respectively. The decrease in  $Q$  as a result of decrease in permeability should be noted.

#### 4.5. Sorption phenomena

The possible sorption of a series of radionuclides in trace amounts onto the chalk has been studied by two distinct different methods: a) batch-type experiments, where crushed chalk samples are equilibrated with a sodium chloride solution, containing the radionuclides, by shaking or b) column-type experiments, where a small sample of the radionuclide solution is injected into the

LC-system (cf. Fig. 1), the column being continuously eluted with the sodium chloride solution (saturated with calcium carbonate) (cf. experimental section).

The radionuclides used for the present sorption studies include four cations ( $^{134}\text{Cs}^+$ ,  $^{60}\text{Co}^{2+}$ ,  $^{85}\text{Sr}^{2+}$ , and  $^{154}\text{Eu}^{3+}$ ) and two anionic species ( $^{36}\text{Cl}^-$  and  $^{99}\text{TcO}_4^-$ ).

Apart from the importance of cesium, cobalt, strontium, and technetium as actual components in nuclear waste, strontium represents group II elements such as barium and radium, whereas cobalt is believed to be a proper representative for other divalent metal ions, e.g. iron and nickel. Europium is included in the study as a reasonable representative for trivalent actinides as americium (III) and plutonium (III), the latter most surely existing as such under the actual conditions within the Erslev chalk formation (cf. section 5) (Skytte Jensen, 1980). It is, on the other hand, not intelligible whether cesium may be regarded as a representative for other monovalent metal ions, such as rubidium, or whether the sorption phenomena observed in the cesium case should be connected specifically to the latter, since rather distinct features connected to cesium sorption have been reported previously (Grim, 1968).

It is well established that the stable oxidation state of technetium in aerated solutions is +7, i.e. technetium appears under such conditions as negatively charged pertechnetate ions ( $\text{TcO}_4^-$ ) (Skytte Jensen, 1980). However, at the actual oxidation potential in the Erslev chalk formation (Eh approx. -0.3; cf. section 5) technetium may appear in the oxidation state +4, as  $\text{TcO}_2^{2+}$ . Furthermore, at pH around 9.0  $\text{TcO}_2^{2+}$  will most efficiently precipitate as  $\text{TcO}(\text{OH})_2$ , which, of course, will be in equilibrium with  $\text{TcO}(\text{OH})_2$  in solution (Skytte Jensen, 1980). Laboratory experiments with these reduced technetium state have not been included.

#### 4.5.1. Batch-type experiments

By the batch-type experiments the sorption of  $^{134}\text{Cs}^+$ ,  $^{85}\text{Sr}^{2+}$ ,  $^{60}\text{Co}^{2+}$ , and  $^{154}\text{Eu}^{3+}$  has been studied. These experiments were carried out for all 21 chalk samples available. Two series of experiments were performed, corresponding to bulk sodium chloride concentrations of 1M and 5M for the equilibrating solution, respectively. Distribution coefficients were determined as described in the experimental section (section 3) and the corresponding retention factors were calculated by Eq. 2.6 adopting the bulk  $\text{CaCO}_3$  density as  $2.7 \text{ g/cm}^3$  and the porosities reported in sec-

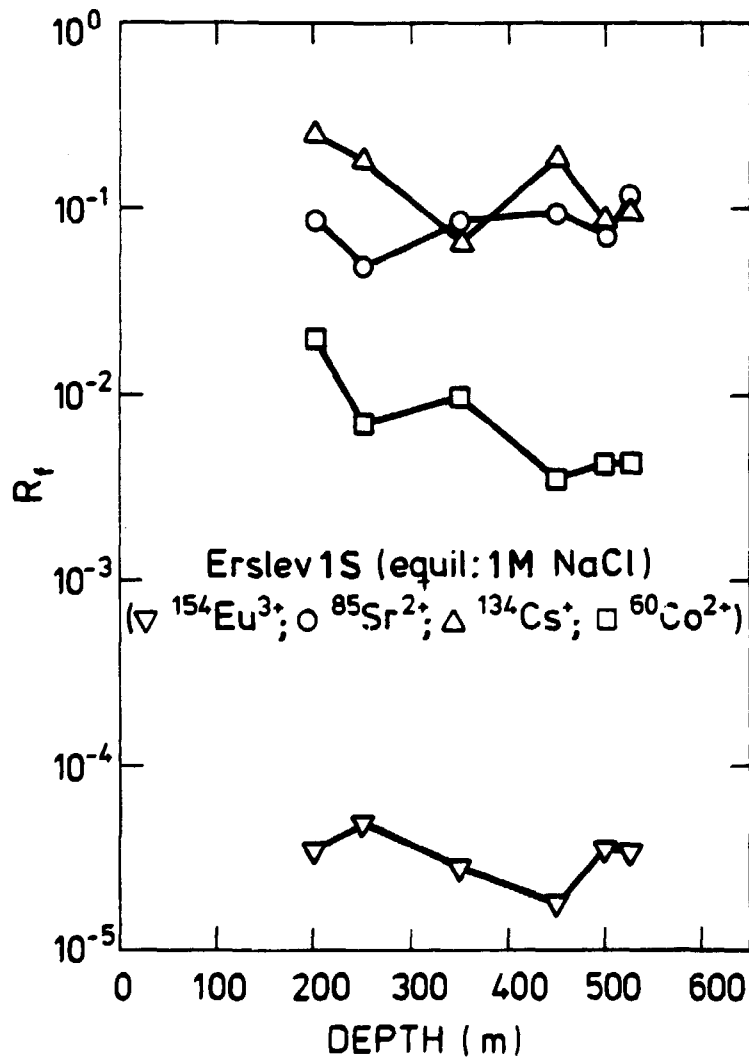


**Fig. 12.** Retention factors as function of depth (Erslev 1s/1M NaCl).

tion 4.2. In Figs. 12 - 19 the results are visualized, the calculated retention factors being depicted as function of depth below ground level.

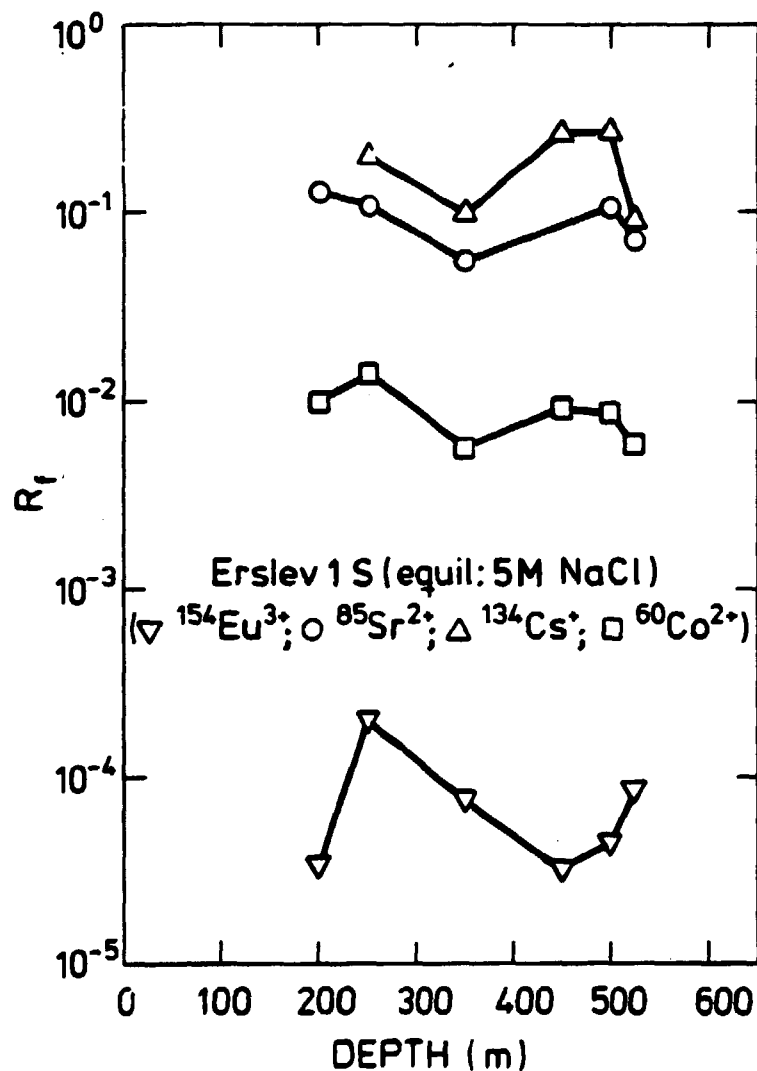


Fig. 13. Retention factors as function of depth (Erslev 1s/5M NaCl).

In accordance with previously obtained experience (Bo and Carlsen, 1981b) values obtained by batch-type experiments are rather scattered. However, a clear-cut pattern is unambiguously recognized concerning the mutual location of the single radionuclides in the " $R_f$  - depth" diagrammes. In addition a slight tendency to decreasing  $R_f$  values with increasing depth is observed.

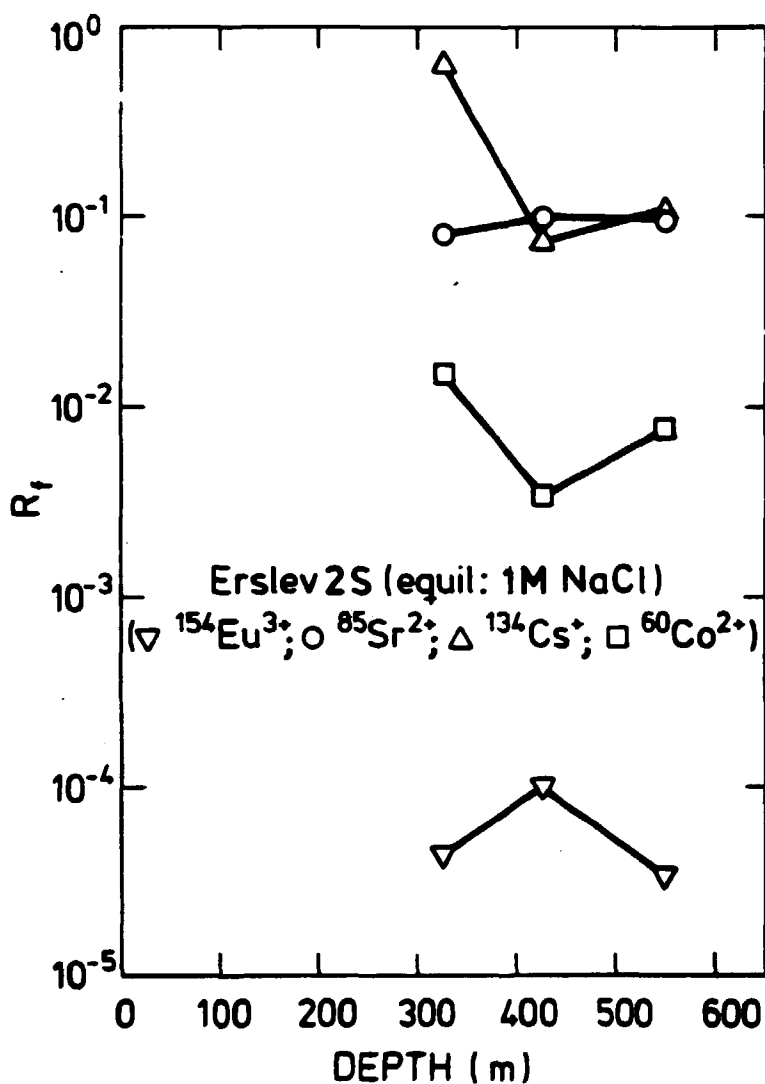


Fig. 14. Retention factors as function of depth (Erslev 2s/1M NaCl).

Most striking, however, is the apparent equality of the four wells. No dramatic changes in the retention factors are observed comparing the single samples. Accordingly, mean values for the retention factors for the single radionuclides (including all 21 samples) and standard deviations are calculated (Table 4). The corresponding mean  $K_D$  values (adopting  $\epsilon = 0.4$  and  $\rho = 2.7$ ) are given in Table 5.

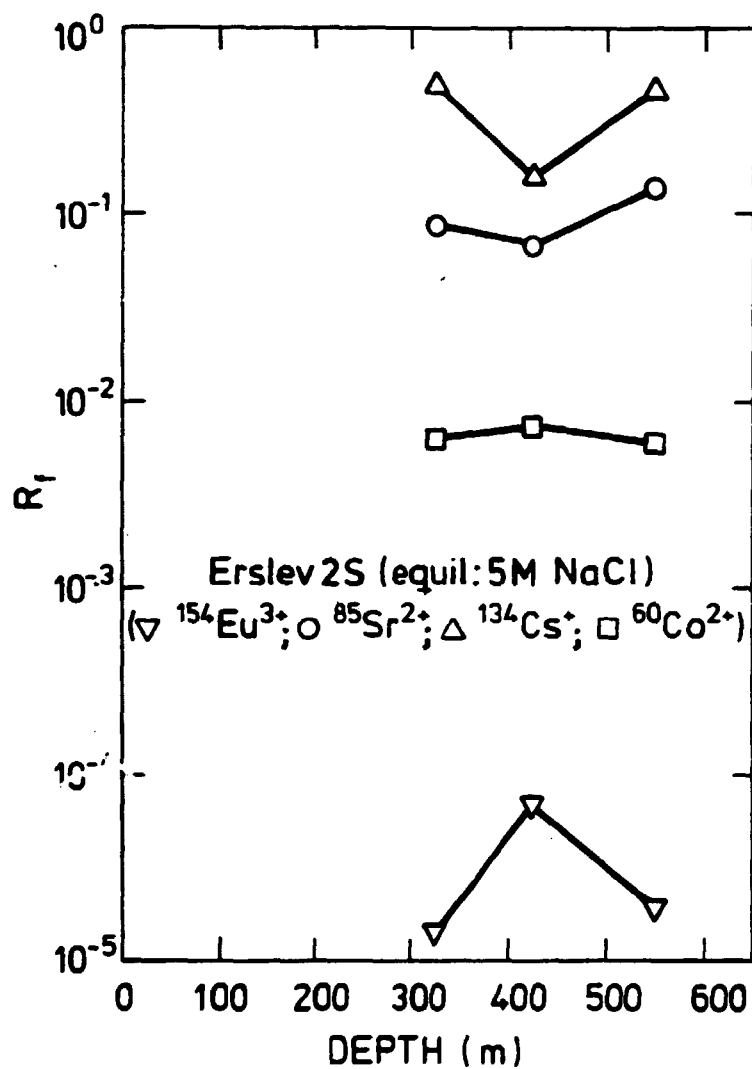


Fig. 15. Retention factors as function of depth (Erslev 2s/5M NaCl).

Table 4. Mean retention factors and standard deviations.

[NaCl]	1M	5M
$R_f(\text{Eu})$	$(5.5 \pm 3.8) \cdot 10^{-5}$	$(5.2 \pm 4.4) \cdot 10^{-5}$
$R_f(\text{Co})$	$(7.8 \pm 4.4) \cdot 10^{-3}$	$(9.0 \pm 4.1) \cdot 10^{-3}$
$R_f(\text{Sr})$	$(8.9 \pm 3.1) \cdot 10^{-2}$	$(9.8 \pm 3.6) \cdot 10^{-2}$
$R_f(\text{Cs})$	$(1.4 \pm 1.3) \cdot 10^{-1}$	$(2.1 \pm 1.3) \cdot 10^{-1}$



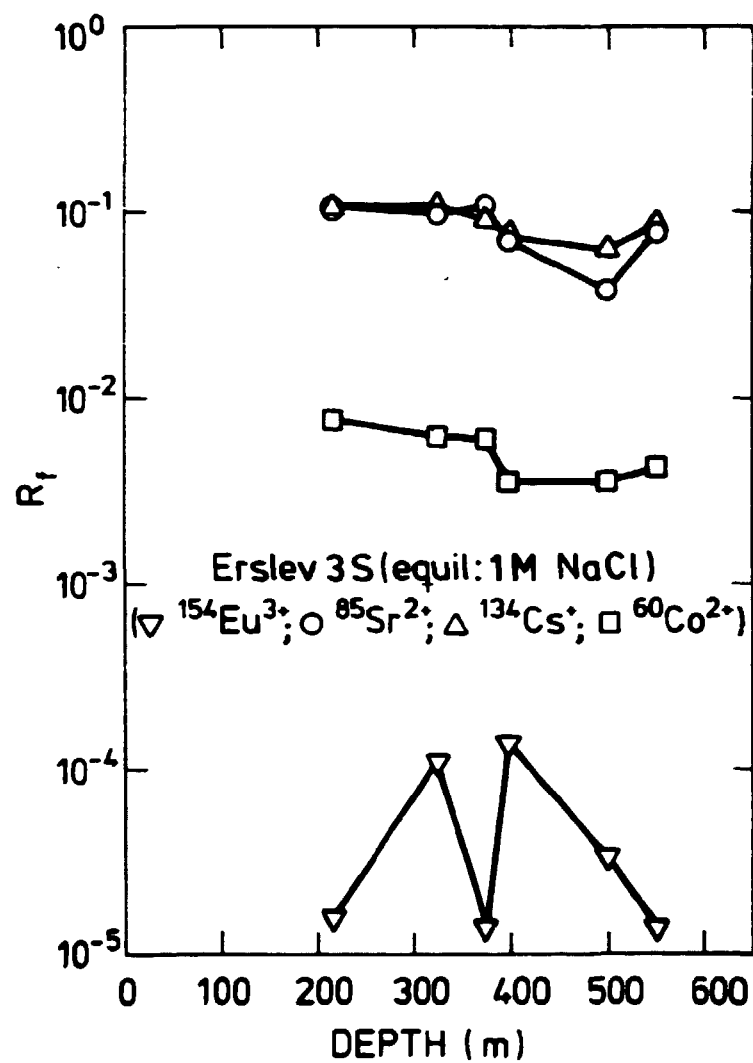
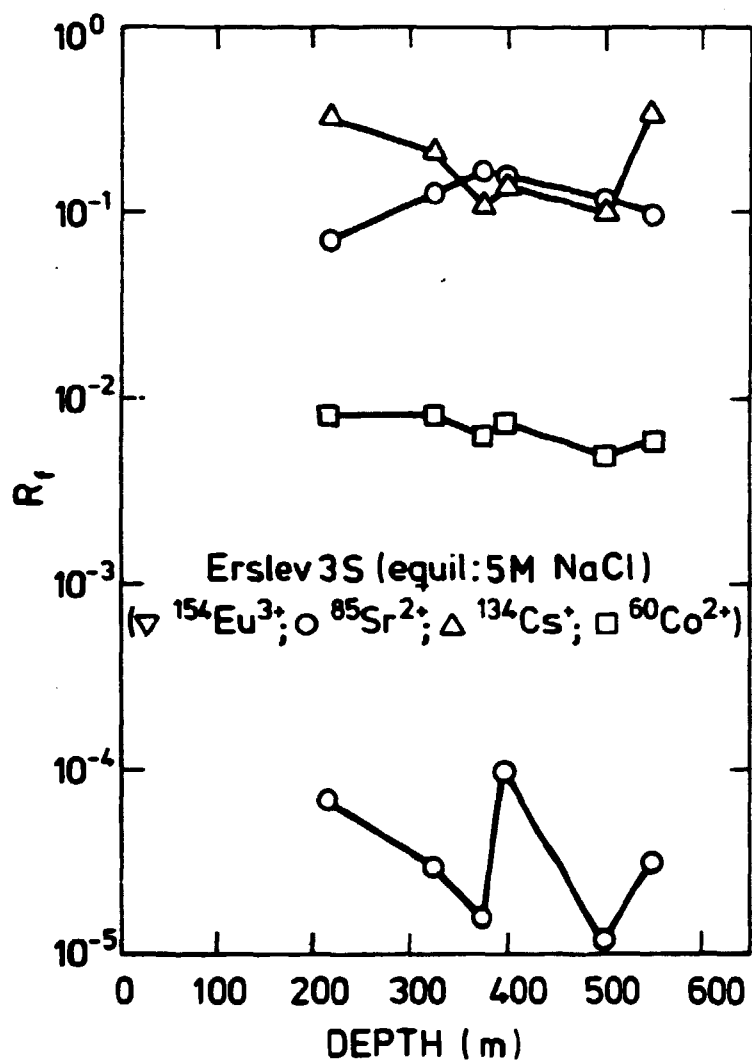


Fig. 16. Retention factors as function of depth (Erslev 3s/1M NaCl).

Table 5. Mean  $K_D$  values.

[NaCl]	1M	5M
$K_D(\text{Eu})$	$4.5 \cdot 10^3$	$4.8 \cdot 10^3$
$K_D(\text{Co})$	$3.1 \cdot 10^1$	$2.7 \cdot 10^1$
$K_D(\text{Sr})$	2.5	2.3
$K_D(\text{Cs})$	1.5	0.9



**Fig. 17.** Retention factors as function of depth (Erslev 3s/5M NaCl).

A slight tendency to increasing  $R_f$  factors (decreasing  $K_D$  values) by increasing bulk sodium chloride concentration is noted. The effects of the bulk salt concentration is further discussed below in connection with the column experiments.

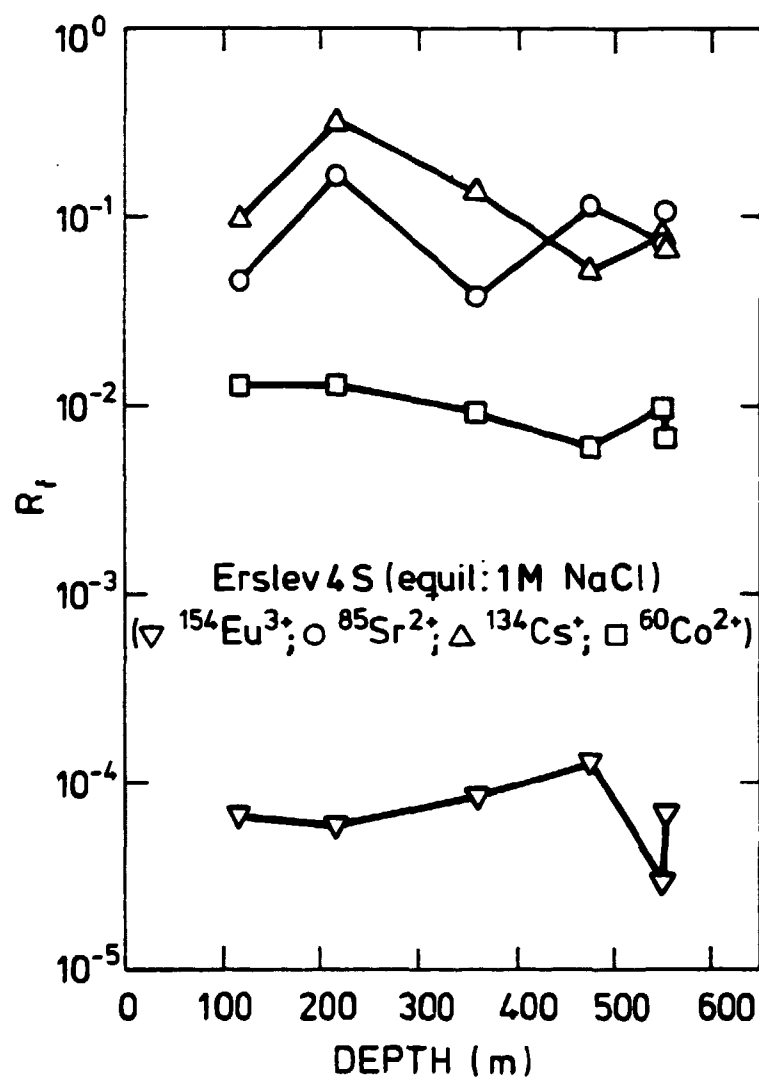


**Fig. 18.** Retention factors as function of depth (Erslev 4s/1M NaCl).

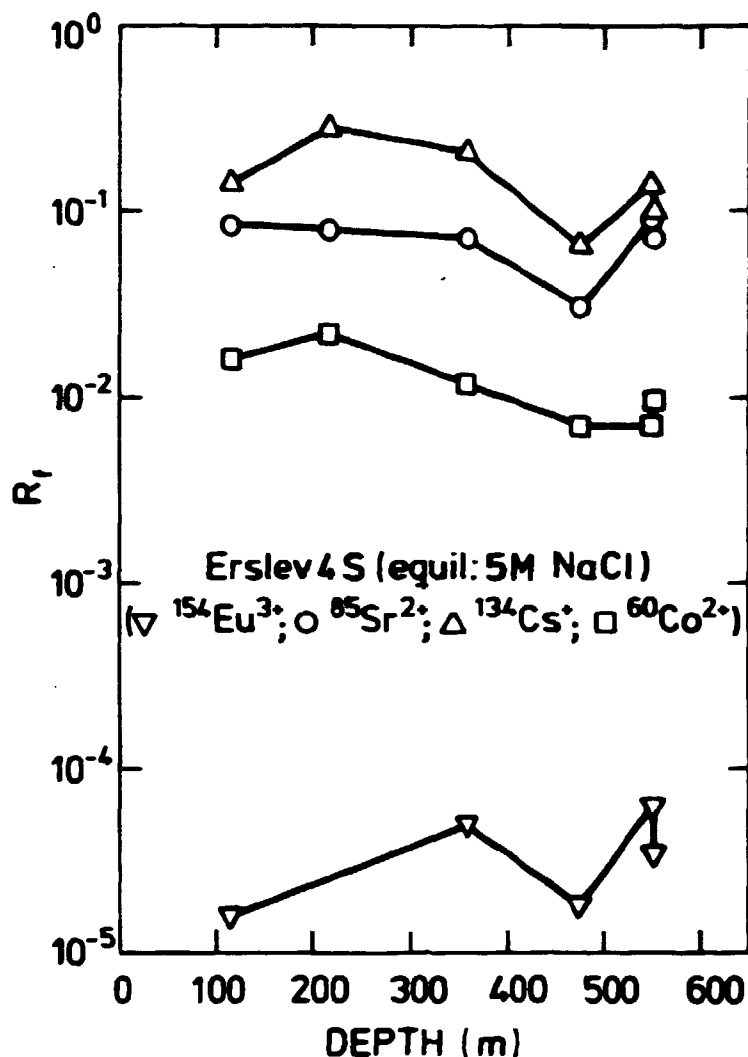


Fig. 19. Retention factors as function of depth (Erslev 4s/5M NaCl).

#### 4.5.2. Column-type experiments

The column-type experiments were carried out by application of the LC-technique. 50  $\mu\text{L}$  samples of ca.  $10^{-3}$  eq/L solutions of NaCl, CsCl,  $\text{SrCl}_2$ , and  $\text{CoCl}_2$  containing trace amounts of  $^{36}\text{Cl}^-$ ,  $^{134}\text{Cs}^+$ ,  $^{85}\text{Sr}^{2+}$ , and  $^{60}\text{Co}^{2+}$ , respectively, and of  $\text{K}^{99}\text{TcO}_4$  were injected and the radioactivity eluted from the columns was detected by a radioactivity monitor (cf. experimental section). The columns were eluted with 0.1, 0.5, 1.0, 2.0, and 4.0 molar sodium chloride solutions, primarily saturated with calcium carbonate. Since  $^{36}\text{Cl}^-$  will not be retarded, the appearance of the

$^{36}\text{Cl}^-$  signal visualizes the passage of the solvent front (corresponding to  $t_0$ ).

In the present study the retention of  $^{134}\text{Cs}^+$ ,  $^{85}\text{Sr}^{2+}$ , and  $^{99}\text{TcO}_4^-$  has been investigated on homogeneous columns, whereas the heterogeneous approach has been applied to  $^{60}\text{Co}^{2+}$  retention.

The determined retention factors for  $^{134}\text{Cs}^+$  and  $^{85}\text{Sr}^{2+}$  for four representative core samples are given in Table 6. No retarding effect of the chalk samples on  $^{99}\text{TcO}_4^-$  was observed.

Table 6. Column-type experiment derived retention factors for  $^{134}\text{Cs}^+$  and  $^{85}\text{Sr}^{2+}$  ( 10 mm homogeneous chalk columns)

	1s-5		4s-3		2s-9		4s-6	
[NaCl]	$^{134}\text{Cs}^+$	$^{85}\text{Sr}^{2+}$	$^{134}\text{Cs}^+$	$^{85}\text{Sr}^{2+}$	$^{134}\text{Cs}^+$	$^{85}\text{Sr}^{2+}$	$^{134}\text{Cs}^+$	$^{85}\text{Sr}^{2+}$
0.5	0.13	0.11	0.12	0.15	0.09	0.11	0.05	0.12
1.0	0.23	0.24	0.26	0.21	0.12	0.08	0.10	0.14
2.0	0.40	0.31	0.38	0.28	0.28	0.26	0.17	0.18
4.0	0.35	0.22	0.51	0.28	0.34	0.18	0.29	0.18

By comparing the values in Table 6 with the average  $R_f$  factors derived from the batch-type experiments (Table 4) it is clear that the column-type experiments give somewhat higher values than do the batch-type, which most probably is to be associated with the crushing of the chalk samples for the latter type of experiments, giving rise to new surfaces. In addition, slow equilibration in the columns may play a role. The consistency between the two different techniques, however, is unambiguously demonstrated in the case of  $^{60}\text{Co}^{2+}$  retardation on the heterogeneous columns. Columns were made with crushed material from the core samples 4s-3 and 4s-6, the chalk being diluted by a factor 12.5 and 15, respectively, by polystyrene spheres (cf. experimental section). The column derived  $R_f$  values (corrected to pure consolidated chalk) were found to be  $1.17 \cdot 10^{-2}$  and  $0.51 \cdot 10^{-2}$ , respectively. The corresponding values obtained in the batch-type experiments were  $1.72 \cdot 10^{-2}$  and  $1.02 \cdot 10^{-2}$ , respectively.

It should be noted (Table 6) that the trend observed in the batch-type experiments, indicating a slightly increased retardation by increasing depth below ground level is refound here.

#### 4.5.2.1. Influence of bulk salt concentration in the eluent

From the data given in Table 6 it is noted that a slight dependence of the bulk salt concentration in the eluent apparently is present. However, the here observed phenomena probably is only minor effects, whereas for more dramatic effects are observed for salt concentrations below 0.5M. In fact, we were unable to produce reasonable chromatograms eluting the columns with salt solutions of concentrations below that level, as the signals became extremely broad in addition to drastically decreased retention factor. It is believed that the retention factors decreases dramatically by further lowering of the salt concentration, in good agreement with the recent investigations of Seitz *et al.* (Seitz *et al.*, 1979), who found extremely small  $R_f(\text{Cs})$  factors in chalk formations. The same is most probably true for other radionuclides. In fact pronounced tailing phenomena are observed in the chromatograms even within the sodium chloride concentration range studied here. In Fig. 20 the eluted  $^{134}\text{Cs}^+$ , as function of time and salt concentration from a 10 mm Erslev 4s-3 column is visualized.

#### 4.5.2.2. Influence of complexing agents

Finally the effect of complexing agents shall briefly be mentioned.

The possible influence of complexing agents was studied by injecting 50  $\mu\text{L}$  samples of  $^{134}\text{Cs}^+$ ,  $^{85}\text{Sr}^{2+}$ ,  $^{60}\text{Co}^{2+}$ , or  $^{154}\text{Eu}^{3+}$  solutions onto a homogeneous 10 mm Erslev 4s-3 column. Immediately after, 50  $\mu\text{L}$  of a Triplex (disodium salt of ethylenediamine tetraacetic acid) was injected and the retention times were then studied. In the case of Triplex as complexing agent we found that  $^{60}\text{Co}^{2+}$  and  $^{154}\text{Eu}$  in fact were eluted with the solvent front, whereas very minor retention of  $^{85}\text{Sr}^{2+}$  is observed ( $R_f \approx 0.95$ ). No influence on the  $^{134}\text{Cs}^+$  retention was observed. We conclude

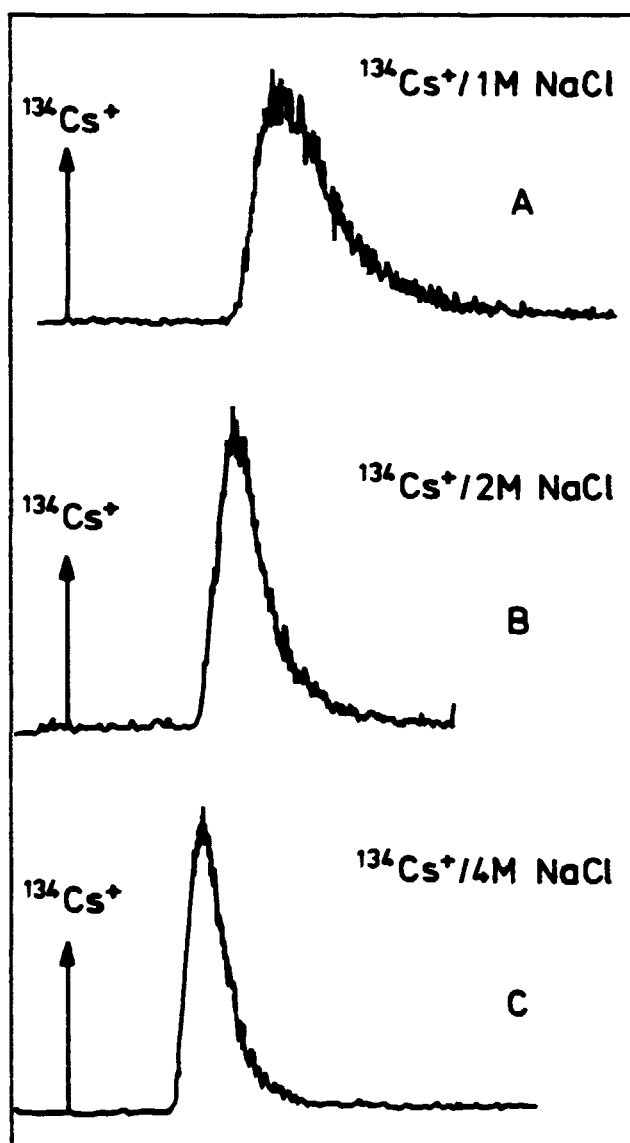


**Fig. 20.** Retention of  $^{134}\text{Cs}^+$  in a 1 cm Erslev 4s-3 column as function of the eluent sodium chloride concentration. (Flow rate: 0.3 mL/min.).

on the basis of these experiments that in the presence of complexing agents the retention of multi-valent radionuclides, such as  $^{60}\text{Co}^{2+}$ ,  $^{85}\text{Sr}^{2+}$ , and  $^{154}\text{Eu}^{3+}$  decreases dramatically, whereas mono-valent metal ions, as  $^{134}\text{Cs}^+$ , not are affected.

## 5. GEOCHEMICAL IMPLICATIONS

The geological formation overlying the top of the Erslev salt dome consists mainly of chalk. The material is very fine grained consisting mostly of skeletons of microorganisms from the cretaceous period. The remains consist mainly of calcite more or less enriched with magnesium (Kinard, 1980 and Chave, 1962); however, in the present case the exact composition of the formation has not been determined.

It has been reported that the presence of magnesium ions in the aqueous phase inhibitates cementing processes in chalk formations (Bjørlykke, 1977). Thus, the increase in magnesium concentration with depth (Solgård and Skytte Jensen, 1981) has accordingly afforded that the major part of the formation consists of rather soft material of high porosity and consequently with a large free surface area pr. unit volume.

### 5.1. Redox and pH conditions in the Erslev chalk formation

Since it has not been possible to collect uncontaminated samples of ground water from the chalk formation to establish redox potentials and pH conditions, a model calculation has been carried out in order to estimate the chemical conditions within the formation.

The analyses of pore water composition has been described in detail elsewhere (Solgård and Skytte Jensen, 1981). The chalk samples were equilibrated for several hours with an artificial aqueous phase before analysis of the liquid phase. Inspection of the analytical data (Solgård and Skytte Jensen, 1981), revealed that the measured concentrations of calcium seem to exceed calculated equilibrium concentrations assuming simple dissolution of  $\text{CaCO}_3$ . Thus, in the present model it has been assumed that within the chalk formation concentrations of different species are determined by an equilibrium between calcium ions in solution, orig-



inating from dissolution of the salt dome and the cap-rock, the latter consisting largely of anhydrite, i.e.  $\text{CaSO}_4$ , and calcite.

The presence of an increased calcium ion concentration in solution influence the calcite solubility as well as equilibria involving carbonate ions. Other salts present in solution are considered to be chemically inactive although contributing to the overall ionic strength. Through out the calculations an average ionic strength equal to 1.0 has been assumed, applying available equilibrium constants.

At an ionic strength equal to 1.0 the relevant equilibrium constants (given in Scheme 5-1) have been reported previously (Smith and Martell, 1976).

Scheme 5-1

$[\text{Ca}^{2+}][\text{CO}_3^{2-}]$	$= 10^{-8.01}$	$= K_s$
$[\text{CaOH}^+]/[\text{Ca}^{2+}][\text{OH}^-]$	$= 10^{0.64}$	$= \beta$
$[\text{CaHCO}^+]/[\text{Ca}^{2+}][\text{HCO}_3^-]$	$= 10^{0.81}$	$= \gamma$
$[\text{H}^+][\text{HCO}_3^-]/[\text{H}_2\text{CO}_3]$	$= 10^{-6.02}$	$= K_1$
$[\text{H}^+][\text{CO}_3^{2-}]/[\text{HCO}_3^-]$	$= 10^{-9.57}$	$= K_2$
$[\text{H}^+][\text{OH}^-]$	$= 10^{-13.79}$	$= K_w$
$[\text{CaCO}_3]/[\text{Ca}^{2+}][\text{CO}_3^{2-}]$	$= 10^3$	$= \delta$

The principle of electroneutrality will in the present case lead to Eq. 5.1

$$[\text{H}^+] + 2[\text{Ca}^{2+}] + [\text{CaOH}^+] + [\text{CaHCO}_3^+] = 2[\text{CO}_3^{2-}] + [\text{HCO}_3^-] + n[\text{X}^{n-}] + [\text{OH}^-] \quad (5.1)$$

where the concentration  $[\text{X}^{n-}]$  corresponds to the equivalents of possible calcium salts (" $\text{CaX}_n$ ", e.g.  $\text{X} = \text{Cl}, \text{SO}_4$ ) dissolved in the aqueous phase. In addition the stoichiometric equation (Eq. 5.2) is valid.

$$\begin{aligned}
 & [\text{Ca}^{2+}] + [\text{CaOH}^+] + [\text{CaHCO}_3^+] + [\text{CaCO}_3] = \\
 & [\text{CO}_3^{2-}] + [\text{HCO}_3^-] + [\text{H}_2\text{CO}_3] + [\text{CaHCO}_3^+] + [\text{CaCO}_3] + n/2[\text{X}^{n-}] \quad (5.2)
 \end{aligned}$$

Combining the equations 5.1 and 5.2 the following expression (Eq. 5.3) is obtained

$$[\text{H}^+] - [\text{CaOH}^+] + [\text{CaHCO}_3^+] + [\text{HCO}_3^-] + 2[\text{H}_2\text{CO}_3] - [\text{OH}^-] = 0 \quad (5.3)$$

Substitution of the expressions given in Scheme 5-1 into Eq. 5.3 affords the following equation (Eq. 5.4)

$$\begin{aligned}
 & [\text{H}^+] - [\text{Ca}^{2+}] \beta K_w / [\text{H}^+] + \gamma K_s [\text{H}^+] / K_2 + K_s [\text{H}^+] / K_2 [\text{Ca}^{2+}] + \\
 & 2K_s [\text{H}^+]^2 / K_1 K_2 [\text{Ca}^{2+}] - K_w / [\text{H}^+] = 0 \quad (5.4)
 \end{aligned}$$

Eq. 5.4 can be solved for  $[\text{H}^+]$  as function of  $[\text{Ca}^{2+}]$ , which allows simultaneous calculation of concentrations of other species present.

In Fig. 21 concentrations of the different species are depicted as functions of total concentration of calcium in solution (i.e.  $c_T = [\text{Ca}^{2+}] + [\text{CaOH}^+] + [\text{CaHCO}_3^+] + [\text{CaCO}_3]$ ). The total concentration,  $c_T$ , calculated in this way corresponds closely to analytical data for calcium concentrations in the aqueous phase within the formation. These concentrations vary between 0.01 and 0.125M (Solgård and Skytte Jensen, 1981). Hence, it is accordingly possible to read the corresponding concentration ranges for other species by application of Fig. 21. The chemical conditions within the formation have been estimated as follows (Scheme 5-2).

According to these data the partial pressure of carbon dioxide within the formation are estimated to be  $10^{-6.5}$  atm.

As mentioned above the redox conditions within the formation has not been measured, due to lack of autentic samples of ground water. However, the observation (*cf.* footnote p. 5) that pyrite, i.e.  $\text{FeS}_2$ , is among the trace minerals found in the formation

Scheme 5-2

RANGE	
pH	8.2 - 8.8
$[\text{CO}_3^{2-}]$	$10^{-6}$ - $10^{-7.2}$
$[\text{HCO}_3^-]$	$10^{-5}$ - $10^{-5.8}$
$[\text{H}_2\text{CO}_3]$	$\approx 10^{-8}$
$[\text{CaCO}_3]$	$\approx 10^{-5}$
$[\text{CaOH}^+]$	$10^{-5.8}$ - $10^{-6.5}$
$[\text{CaHCO}_3^-]$	$10^{-5.8}$ - $10^{-6.5}$

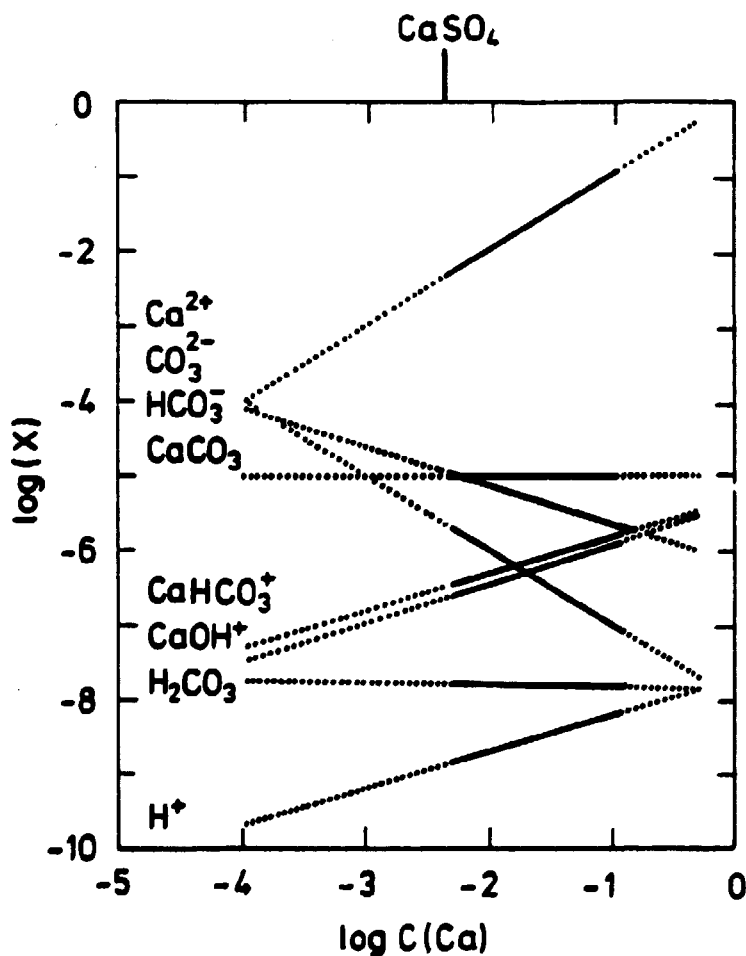


**Fig. 21.** Equilibrium concentrations of  $\text{Ca}^{2+}$ ,  $\text{CaOH}^+$ ,  $\text{CaHCO}_3^-$ ,  $\text{CaCO}_3$ ,  $\text{CO}_3^{2-}$ ,  $\text{HCO}_3^-$ ,  $\text{H}_2\text{CO}_3$ , and  $\text{H}^+$  as function of total soluble calcium in the system calcite/" $\text{CaX}_n$ ". Equilibrium constants apply to the condition of ionic strength equal to 1.0. Full drawn lines correspond to the range found in the core samples.

apparently fix the possible redox potential within rather narrow limits close to the equilibrium line between  $\text{SO}_4^{2-}$  and  $\text{HS}^-/\text{S}^{2-}$  in a Eh-pH diagram (Fig. 22). The possible pH conditions calculated (Scheme 5-2) lead to an expected redox potential at approximately  $-0.3 \pm 0.1$  volts, which identifies the area within the Eh-pH diagrams most probably corresponding to the actual conditions to be found in the Erslev chalk formation.

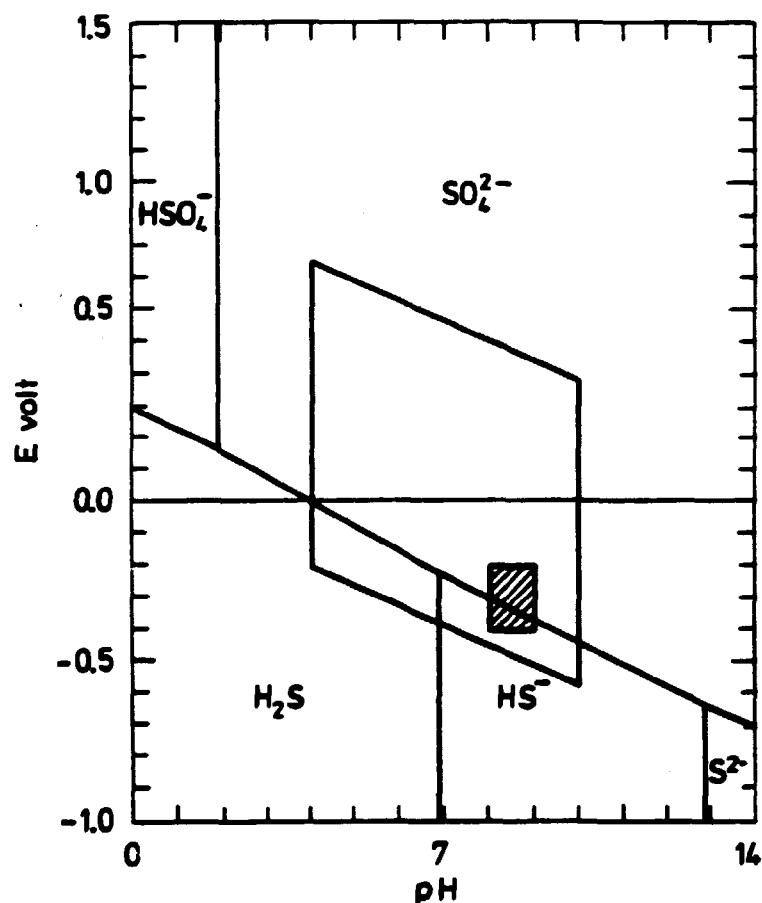


Fig. 22. The hatched area indicates the expected chemical conditions within the Erslev chalk formation.

## 5.2. Geochemistry of radionuclides

Examination of the stability diagrams previously presented in the report "The Geochemistry of Radionuclides with Long Halflives" (Skytte Jensen, 1980), afford the speciation of the transuranium

elements as well as technetium under the above established conditions. The corresponding maximum solubilities of the single elements can be read from the diagrams displaying iso-concentration curves within the Eh-pH field (Skytte Jensen, 1980).

The diagrams reveal that neptunium should be found in solution in very minor concentrations only (in the order of  $10^{-12}$  M) apparently as  $\text{Np}(\text{OH})_3^+$  in equilibrium with the very slightly soluble  $\text{NpO}_2$ .

Plutonium apparently appears in the oxidation state +3 as  $\text{Pu}(\text{HO})^{2+}$  also in very low concentrations (in the order of  $10^{-12}$  M) in equilibrium with the very slightly soluble  $\text{PuO}_2$ .

Americium will, as plutonium, exist in the oxidation state +3 as  $\text{Am}(\text{OH})^{2+}$ , however, in concentrations up to  $10^{-4}$  M in equilibrium with the slightly soluble  $\text{Am}(\text{OH})_3$ . If, on the other hand, it can be assured that the solubility product of  $\text{Am}_2(\text{CO}_3)_3$  is comparable to that of  $\text{Eu}_2(\text{CO}_3)_3$ , i.e.  $10^{-33}$ , the maximum solubility of americium can be calculated to lie within the same range in the given system.

For technetium the tetravalent undissociated species  $\text{TcO}(\text{OH})_2$  will be dominant under the actual conditions and will accordingly exist in solution in very low concentrations only, in the order of  $10^{-7}$  M. The solid phase in equilibrium with the aqueous solution apparently consists of the slightly soluble  $\text{TcO}_2$ .

The retention experiments discussed above (cf. section 4.5) unambiguously demonstrate that all cationic species, including  $\text{Cs}^+$ ,  $\text{Sr}^{2+}$ ,  $\text{Co}^{2+}$ , and  $\text{Eu}^{3+}$  more or less are adsorbed by the chalk, whereas no retarding effect on anionic species like  $\text{Cl}^-$  and  $\text{TcO}_4^-$  are observed, suggesting ion-exchange as a possible mechanistic approach, although simple precipitation reactions, as indicated above, in addition may play an important role, especially in the case of europium.

Ion exchange phenomena could a priori be ascribed to minor amounts of clay material present in the chalk; on the other hand, the relative insensitivity of the sorption on the bulk salt con-

contraction, at least in the range above 0.5M, suggests that the more specific surface binding mechanisms operate. It is known that most mineral surfaces, including that of calcite, acquires a negative charge at increased pH-values (Stumm and Morgan, 1970); hence, they become capable of adsorbing or incorporating cationic species into their surface layers. The available surface for adsorption of the present type of chalk may well approach several square metres pr. gram and accordingly calcite itself may well be the effective sorbing material responsible for the experimental results given above. Supplementary column-type experiments to study e.g.  $^{134}\text{Cs}^+$  retention on pure, precipitated  $\text{CaCO}_3$  were carried out. The results obtained unequivocally confirm that calcium carbonate most surely is the retarding material. In 1M sodium chloride solution (as eluent) the following results were obtained:  $\text{CaCO}_3$ ,  $R_f(\text{Cs}) = 0.23$ , Erslev 4s-3,  $R_f(\text{Cs}) = 0.26$ , Erslev 1s-5,  $R_f(\text{Cs}) = 0.23$  (cf. Table 6).

Of the ions investigated, cesium, strontium, and technetium themselves are important radionuclides in the nuclear waste. The trivalent europium can be considered as a proper model compound for the trivalent actinides, in the present case  $\text{Am}^{3+}$  and  $\text{Pu}^{3+}$ , since experiments as well as theory have shown similar chemical reactions for these ions. Additionally, rather close values for different equilibrium constants have been estimated (Comprehensive Inorganic Chemistry, 1973).

## 6. CONCLUSIONS

In the present study chalk samples from Erslev, Mors, Denmark have been investigated predominantly by a liquid chromatographic technique in order to establish permeability, porosity, dispersion-, diffusion-, and sorption characteristics for the chalk formation. In addition porosities have been estimated by density measurements and sorption characteristics by batch type experiments.

It must strongly be emphasized that only 21 samples (6 from Erslev 1s, 3 from Erslev 2s, 6 from Erslev 3s, and 6 from Erslev 4s) have been available for these investigations, however, a rather clear-cut picture has been developed.

Although the samples in general exhibited high porosities, around 0.4, they were found to be rather impermeable, as the permeabilities were found in the range from  $10^{-6}$  to  $10^{-8}$  cm/sec. The permeabilities appear to decrease with increasing depth below ground level.

The flow-dispersion was, for experimental reasons, determined at flow rates down to ca. 0.03 mL/min only, which apparently is very much higher than the actual flow conditions within the formation. The dispersion coefficients were determined to ca.  $6 \cdot 10^{-5}$  cm<sup>2</sup>/sec, close the diffusion coefficient in pure water. However, it is believed that this value, due to the low permeability, may be up to several orders of magnitude higher than the actual effective diffusion coefficient within the chalk.

The apparent diffusion coefficients for  $^{22}\text{Na}^+$  in two representative chalk samples from the Erslev formation was determined. The actual magnitude was found to be up to ca.  $10^3$  times lower than the corresponding diffusion coefficient in pure water.

It was found that the chalk exhibited a retarding effect on cationic species such as  $\text{Cs}^+$ ,  $\text{Sr}^{2+}$ ,  $\text{Co}^{2+}$ , and  $\text{Eu}^{3+}$ , whereas anionic species as  $\text{Cl}^-$  and  $\text{TcO}_4^-$  were found to move with the water front, i.e. without retardation.

The likely geochemistry of radionuclides within the formation has been discussed, leading to the conclusion that even in cases of moderate water flows through the chalk formation, migration of actinide cations, as  $\text{Am}^{3+}$  and  $\text{Pu}^{3+}$  effectively will be retarded. Due to the extension of the Erslev chalk formation complementary to its impermeability it seems probable that migration to the surface may be dominated by diffusion.

## ACKNOWLEDGEMENTS

This report has been worked out according to the agreement between Risø National Laboratory and ELSAM/ELKRAFT concerning advisory assistance from Risø to ELSAM/ELKRAFT's management project, Phase 2. The authors are indebted to Mrs. L. Halby and Mrs. G. Larsen for valuable technical assistance.

## REFERENCES

- ATKINS, P.W. (1978). Physical Chemistry (Oxford University Press, Oxford) Chapter 25.
- BECK, R.E. and SCHULTZ, J.S. (1970). Science 170, 1302-5.
- BJØRLYKKE, K. (1977). Sedimentologi, Stratigrafi og Oliegeologi (Universitetsforlaget, Bergen) 236 pp.
- BO, P. and CARLSEN, L. (1981a). DIPMIG- A computer program for calculation of diffusive migration of radionuclides through multibarrier systems. Risø -M-2262. 33 pp.
- BO, P. and CARLSEN, L. (1981b). European Appl. Res. Rept.-Nucl. sci. Technol. 3, 813-73.
- CHAVE, K.E. (1962). Limnol. Oceanog. 7, 218-23.
- COMPREHENSIVE INORGANIC CHEMISTRY (1973). Vol. 5. Actinides. Ed. by J.C. Bailar, Jr., H.J. Emeléus, Sir Ronald Nyholm and A.F. Trotman-Dickenson (Pergamon Press, Oxford).
- DAHL, N.J. (1969). Grundvandbevægelse (Teknisk Forlag, Copenhagen) P. 29.
- GRIM, R.E. (1968). Clay Mineralogy (McGraw-Hill, New York) 220-222.
- HARNED, H.S. and OWEN, B.B. (1963). The Physical Chemistry of Electrolytic Solutions. 3. ed., 2. pr. (Reinhold, New York) American Chemical Society. Monograph Series; 137. 803 pp.
- KINARD, W.F. (1980). J. Chem. Ed. 57, 783-4.
- MARTELL, A.E. and SMITH, R.M. (1976). Critical Stability Constants. Vol. 4. Inorganic Complexes (Plenum Press, New York).



- MEARES, P. (1968). In: Diffusion in Polymers. Ed. by J. Crank and G.S. Park (Academic Press, London) Chapter 10.
- SEITZ, M.G., RICKERT, P.G., FRIED, S., FRIEDMAN, A.M. and STEINDLER, M.J. (1979). Nucl. Technol. 44, 284-96.
- SKYTTE JENSEN, B. (1980). The Geochemistry of Radionuclides with long half-lives. Risø-R-430. 53 pp.
- SOLGARD, P. and SKYTTE JENSEN, B. (1981). Chemical Analysis of Pore Water in Chalk Samples from Erslev, Mors, Denmark. Risø Chemistry Department. Contribution to the ELSAM/ELKRAFT management project, Disposal of High-Level Waste from Nuclear Power Plants in Denmark, Phase 2. Salt Dome Investigations. Volume 2. Geology.
- STUMM, W. and MORGAN, J.J. (1970). Aquatic Chemistry (Wiley, New York) 585 pp.
- YAU, W.W., KIRKLAND, J.J. and BLY, D.D. (1979). Modern Size -Exclusion Liquid Chromatography (Wiley, New York) P. 59.

**Sales distributors:**  
**Jul. Gjellerup, Sølvgade 87,**  
**DK-1307 Copenhagen K, Denmark**

**Available on exchange from:**  
**Risø Library, Risø National Laboratory,**  
**P. O. Box 49, DK-4000 Roskilde, Denmark**

**ISBN 87-550-0785-6**  
**ISSN 0106-2840**